Magnetism, structure, and morphology of ultrathin Fe films on Cu₃Au(100)

B. Feldmann, B. Schirmer, A. Sokoll, and M. Wuttig

Institut für Grenzflächenforschung und Vakuumphysik, Forschungszentrum Jülich D-52425 Jülich, Federal Republic of Germany

(Received 3 July 1997)

The magnetic, structural, and morphological properties of ultrathin Fe films on Cu₃Au(100) have been investigated by low-energy electron diffraction including I/V measurements, Auger electron spectroscopy, medium-energy electron diffraction, and magneto-optic Kerr effect. The main aim of these studies was to establish the correlation between film structure and magnetism. For this purpose both films deposited at 300 K (RT) and at 150 K (LT) followed by subsequent annealing to 300 K were investigated. Above about 1 monolayer (ML), the films exhibit a perpendicular magnetization, which switches at 3.2 ± 0.2 ML for LT and 2.3 ± 0.2 ML for RT films in-plane. The reduction of the switching thickness from perpendicular to in-plane with growth temperature is caused by an interdiffusion at the Fe film/substrate interface. At somewhat larger thickness a structural transition is observed. This structural transition is not related to the magnetic reorientation. Contrary to other studies no evidence is found for any fcc iron modification. We rather conclude that above 5 ML, the iron film transforms from strained to unstrained bcc(100) Fe. [S0163-1829(98)03802-8]

I. INTRODUCTION

By deposition of ultrathin films it is possible to stabilize new materials with properties, which deviate from the corresponding bulk crystals. One aim of the study of thin-film properties is to exploit them for new applications. To tailor films with specific properties, the knowledge about the correlation between the magnetic, structural, and morphological properties is required. Ultrathin Fe films are particularly suited for an investigation of this correlation, because Fe can exist in a ferromagnetic (FM) bcc, FM fcc or antiferromagnetic (AF) fcc modification.[1] Epitaxially grown Fe films on Cu(100) (lattice parameter $a = 3.61$ Å) attracted much attention because the misfit (f) for the antiferromagnetic fcc Fe phase ($a = 3.58$ Å, $f = -0.8\%$) (Ref. 2) and the ferromagnetic fcc Fe phase ($a = 3.66$ Å, $f = 1.3\%$) is small. Both modifications[3–6] have been stabilized by epitaxial growth on a Cu(100) substrate. FM fcc Fe can be grown up to approximately 4.5 monolayers (ML). The quantitative structure determination of the phase revealed that FM fcc Fe is unstable against shears in the fcc[011] direction and is only stabilized by the Cu substrate.[3] This result supports theoretical calculations,[7] which predicted an instability of this phase. In order to investigate the strain-dependent properties of this phase, we chose Cu₃Au(100) ($a = 3.745$ Å) as the substrate, which should allow to expand the in-plane and contract the interlayer distances of a pseudomorphic fcc Fe-film. This substrate has the advantage, that the misfit for the FM phase ($f = -2.3\%$) is smaller than for the AF ($f = -4.6\%$) and bcc(100) phase ($f = 7.7\%$). Hence the growth of FM fcc(100) Fe might be enabled.

For substrates with an even larger lattice parameter, on the contrary, the misfit for the bcc modification of iron decreases and the misfit for the fcc iron modification increases. Hence, on those substrates which include Au(100) and Ag(100), one expects the stabilization of bcc iron instead of fcc iron. This is in line with a number of previous studies.[8,9] Hence, Cu₃Au(100) should be a particulary interesting substrate for the growth of iron films. Indeed a number of previous studies come to the conclusion that fcc iron grows on Cu₃Au(100) at small thickness.[10–12] With increasing film thickness a transition to unstrained bcc iron is observed. However, up to this point, the evidence for an fcc iron phase has been mainly derived from a kinematic analysis of low-energy electron diffraction (LEED) I/V curves for the (0,0) beam rather than a full-dynamical LEED analysis for several beams. The latest study which followed the kinematical approach was performed by Lin *et al.*[12] These authors correlated the observed magnetic reorientation with a change in the LEED I/V curve and changes in the scanning tunneling microscopy (STM) images with growing film thickness. They concluded that the magnetic reorientation is closely related to a structural transition from fcc(100) to bcc(100) iron. Hence, this scenario would closely resemble the behavior of iron films deposited on Cu(100). This is clearly an interesting and important finding since it extends our knowledge about the limits of metastable epitaxy.

To confirm this interesting observation and to help develop a detailed understanding of the correlation of magnetic, structural, and morphological properties we have studied Fe films on a Cu₃Au(100) crystal. This study finds rather conclusive evidence that the correlation of structure and magnetism for this system differs considerably from several conclusions of previous investigations.

In the next section the experimental setup will be described. Section III is divided into the presentation of the morphological (A), magnetic (B), and structural (C) properties. In Sec. IV we correlate the properties (A) and compare them to previous results (B). Section V contains a short summary.

II. EXPERIMENTAL

The experiments were performed in an ultrahigh-vacuum chamber designed to correlate magnetism, structure, and morphology of ultrathin films. Since the apparatus has already been described elsewhere,[13] only a brief description of the system will be given here. The chamber is equipped with several facilities for the preparation and analysis of thin films and surfaces. The substrate was a polished Cu₃Au(100)

single crystal, approximately 7 mm in diameter and 2.5 mm thick. The surface is oriented to within 0.1° of the surface normal. It was cleaned by Ar-ion sputtering at room temperature and at 490 K for 10 min afterwards. Subsequently the sample was annealed at 770 K for 5 min to allow a smoothening of the surface. Then the sample was held for 20 min at 630 K to order the $Cu_3Au(100)$ alloy surface, which exhibits an order-disorder transition at 660 K. After this treatment contamination levels were below the Auger detection limit (<2 at. %) and LEED showed a sharp pattern typical for the Cu_3Au surface. Due to the different atomic form factor of Cu and Au atoms, additional spots are visible in LEED for the chemically ordered $Cu_3Au(100)$ surface, which are not evolving for unreconstructed fcc(100) surfaces of pure metals. In the notation of this surface, the additional spots are located at $(m+\frac{1}{2}, n+\frac{1}{2})$, $(m,n=0,1,2,3,\dots)$ positions.

Fe was evaporated from a small disk of high purity (99.99%). The pressure rise during Fe deposition was typically below 1×10^{-8} Pa. After the source was turned off it quickly dropped to a base pressure of 4×10^{-9} Pa. The resulting contamination level of the Fe films was below 2%. Deposition rates between 0.3 and 2 ML/min were used. The film growth was monitored by measuring the medium-energy electron-diffraction (MEED) intensity during deposition. For Fe films grown at room temperature, the MEED curves of the (0,0) beam show weak oscillations superimposed on a descending slope up to 3 ML. However, the $(1,\bar{1})$ beam exhibits more pronounced oscillations with constant periodicity up to 6 ML (see Fig. 2). This allows a thickness determination with a precision of 8% and enabled a calibration of the Auger intensity ratios of the Fe (703 eV) and Cu(920 eV) peaks. Our Auger calibration for $Fe/Cu_3Au(100)$ is in excellent agreement with the Auger intensity ratio obtained previously for Fe/Cu(100) after correcting for the reduced Cu density in $Cu_3Au(100)$ as compared with Cu(100). This gives further support for our thickness determination. Fe films were grown with a homogeneous thickness on the $Cu_3Au(100)$ sample or with a wedgelike thickness distribution. The thickness profile of the film was determined by the Auger intensity ratios, which were taken at different positions of the wedge. This allowed an assignment of the film properties to thickness.

In order to investigate structural properties, the LEED pattern was observed and spot profiles were measured in different crystallographic directions. LEED I/V curves were taken for a quantitative, full-dynamical analysis. A comparison of I/V curves with analyzed spectra was used to detect changes of structural properties. Furthermore LEED was employed to investigate the film morphology by observing the energy dependence of the peak width for certain LEED beams.

Magnetic properties of the film were characterized using the magneto-optic Kerr effect (MOKE). The light source was a He-Ne Laser with a wavelength of 632.8 nm. Hysteresis loops were recorded in longitudinal and polar geometry employing a polarization modulation technique. The maximum field which could be applied was 1050 Oe. The dependence of the susceptibility on temperature was measured according to Berger et al.[14] to determine the Curie temperature.

III. RESULTS

For Fe films grown on a Cu(100) single crystal it was shown[1,15] that the properties are sensitively dependent on the preparation conditions, such as the deposition temperature. Interface properties like roughness and interdiffusion of substrate and deposit atoms can be modified by the preparation conditions. Segregation is another effect which could influence the film properties. In principle, three factors[16] determine the segregation of substrate atoms. These are the size of the atoms, the surface free energy and the tendency to form an alloy. Au atoms are larger in size than Fe atoms, which supports the tendency of Au atoms to segregate to the surface. Due to the smaller surface free energy of Au (1.5 J/m^2) and of Cu (1.78 J/m^2) than of bcc Fe (2.41 J/m^2),[16] a covering of the film surface with substrate atoms is preferred. Finally, the binary phase diagrams of Fe and Au and of Fe and Cu (Ref. 17) show a negligible tendency for a solid solution of Au and Cu in Fe and no bulk alloy formation at the investigated temperatures. This implies that predominantly Au atoms may segregate to the film surface upon annealing. The segregation of substrate atoms may also change the Fe-substrate interface, because Fe atoms may occupy the subsurface sites which are created by the segregation of Au and to a lesser extent Cu atoms. Therefore we investigated for comparison the properties of films deposited at 300 K [room temperature (RT)] and at 150 K [low temperature (LT)]. The films deposited at 150 K were subsequently annealed at 300 K for 10 min to improve the structural order and to smooth the film surface.

A. Morphology

First of all we tried to evaluate to what extent interdiffusion and/or segregation of substrate atoms influence the film properties. For this purpose, the intensity of several Auger transitions at low energy (Fe 47 eV, Cu 60 eV, and Au 69 eV) and at higher energy (Fe 703 eV and Cu 920 eV) was measured after deposition at 300 K and the ratios of different peaks were determined. Subsequently the temperature was raised in steps of 30 K. After 20 min at constant temperature the Auger intensity ratios were determined again. A change of the Auger intensity ratio after such an annealing step at a certain temperature is indicative of interdiffusion and/or segregation. At the low thicknesses investigated, the Fe 703 eV / Cu 920 eV ratio remained rather constant, whereas the low-energy Auger intensity ratios changed at temperatures, T_{Diff}, that led to a diffusion of substrate atoms to the film surface. These temperatures are shown in Fig. 1. As expected, the tendency for substrate atoms to diffuse decreases with growing thickness. Au diffuses at considerably lower temperatures than Cu within the investigated thickness regime. A further indication for a predominant diffusion of Au atoms is that the Au 69 eV peak decreases more slowly upon growing thickness than the Cu 60 eV signal. Whereas the Cu peak vanishes at 1.8 ML, a Au peak can be detected up to 4.4 ML. For this reason it cannot be excluded that a diffusion of Au atoms to the film surface influences the film properties up to 4.4 ML for RT preparation. At larger thickness no diffusion of substrate atoms to the film surface could be detected even after annealing to 573 K.
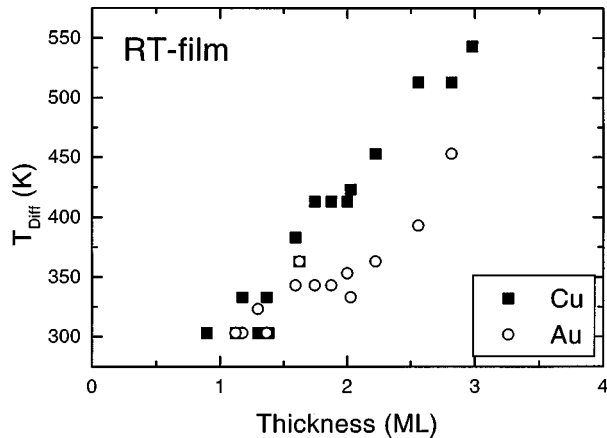
FIG. 1. Thickness dependence of Cu (solid squares) and Au (open circles) diffusion to the Fe film surface. T_{Diff} is the temperature that led to diffusion. Temperatures, at which no diffusion was observed, are 30 K below these values. See text for further details.

Since T_{Diff} reaches a value of 300 K below 2 ML, a segregation of substrate atoms to the film surface influences the film properties already during RT preparation. To avoid this diffusion at low thickness, Fe was deposited at 150 K. Subsequently, the dependence of the Auger peaks on thickness before and after annealing to 300 K was evaluated. The Fe/Cu, Fe/Au, and Cu/Au intensity ratios do not change considerably upon annealing. Both the Cu and Au peak vanish at nearly equal thicknesses, namely 1.6 and 1.9 ML. Hence, a segregation of Cu and Au is negligible for low temperature preparation.

For a complete characterization of the growth, the MEED intensity of several spots was measured simultaneously during deposition. Both the growth mode and the film structure influence the MEED intensity.[17] Furthermore the slope of the curves is dependent upon the scattering conditions.[13] Therefore, one has to be cautious with a straightforward interpretation of MEED curves. The intensity of the $(\frac{1}{2},\frac{1}{2})$ beam, which is caused by the ordered arrangement of Au and Cu atoms, decreases exponentially and vanishes for both growth temperatures after deposition of 1.5 ML. The intensities of the $(0,0)$ spot for growth at 300 and 150 K and the $(1,\bar{1})$ spot at 300 K are shown in Fig. 2. During growth at 300 K, the intensity of the $(1,\bar{1})$ beam, which is diffracted nearly parallel to the film surface, increases up to 1 ML due to the growing disorder of the surface. It exhibits a shoulder at 1 ML and clear oscillations up to 6 ML. The occurrence of these oscillations indicates an oscillation of the step density upon deposition. Above 6 ML, both the $(0,0)$ and $(1,\bar{1})$ beam exhibit a continuously decreasing intensity up to 10 ML. The intensity of the $(0,0)$ beam increases again above 10 ML for RT films. However, for LT films the intensity of the $(0,0)$ beam has its absolute minimum already at 5 ML, before it starts to increase again.

The change of the MEED intensity is also accompanied by a distinct change of the MEED pattern. With growing thickness we observe a reduction of the spot intensity and an increase in spot size. Above a minimum in spot intensity new extra spots develop which increase in intensity with growing thickness. This behavior is observed both for RT and LT
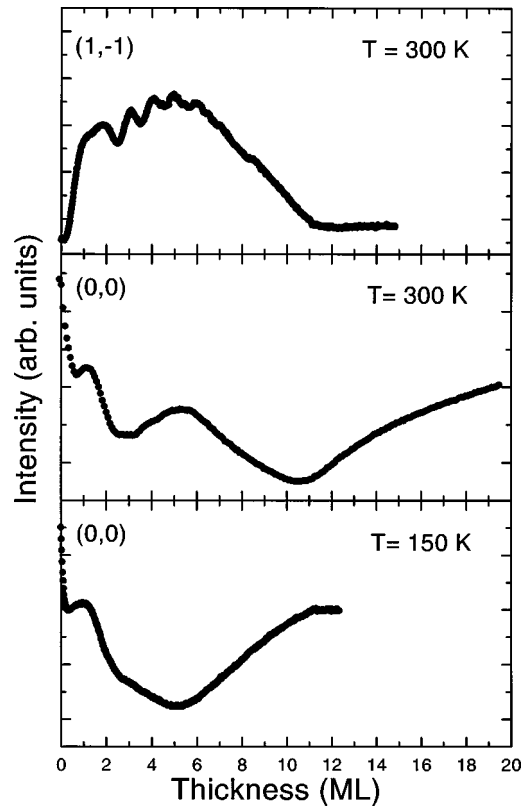

FIG. 2. MEED curve of the $(1,\bar{1})$ and $(0,0)$ spot intensity during deposition at 300 and 150 K. The thickness was calibrated by an evaluation of the MEED oscillations which can be observed in the $(1,\bar{1})$ beam. The curves were recorded with an electron energy of 3 keV and an angle of incidence of 81.4° against the sample normal (out of phase condition). The azimuthal angle was chosen 5.5° off the [001] direction.

preparation, but the thicknesses where characteristic changes are found differ for these two preparation conditions.

One might argue that Au segregation at RT is responsible for the difference in film growth as evidenced by the MEED curves. The first evidence against this assumption is the fact that the MEED intensity curve of films deposited at 420 K is similar to films grown at RT, although Au is able to segregate in a larger amount to the film surface. To suppress Au segregation during deposition at 300 K, the following film preparation was chosen. Initially 2 ML were deposited at LT and annealed to 300 K to avoid segregation of Au. Subsequently, Fe layers were deposited at 300 K. Since the MEED curves for this film closely resemble the behavior of RT films, the segregation of Au is not responsible for the different MEED curves of RT and LT films.

B. Magnetic properties

For both preparation conditions, a sequence of polar and longitudinal hysteresis loops were recorded at 166 K. The Kerr ellipticity at saturation (M_s) and at remanence (M_r) as well as the coercive force (H_c) were determined for different thicknesses. The results for (M_s) and (H_c) are shown in Figs. 3 and 4. The data for (M_r) (not shown) closely resemble the behavior of (M_s). At first sight the development of the magnetic properties seems to be fairly similar for LT
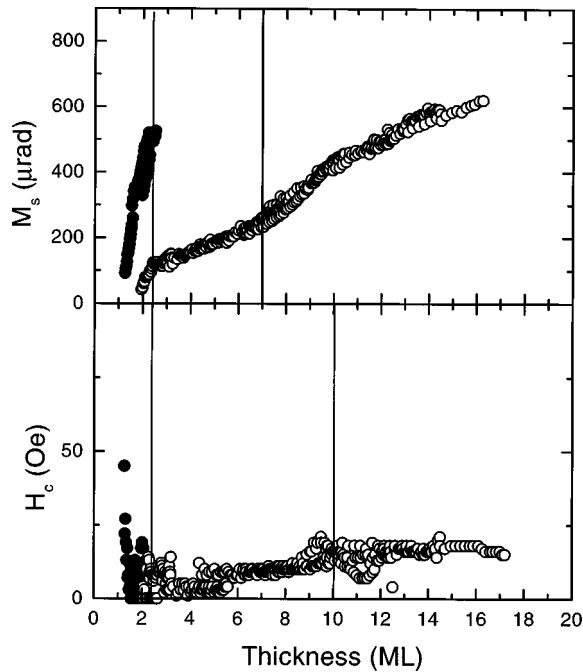
FIG. 3. Thickness dependence of the Kerr ellipticity at saturation M_s and of the coercive force H_c for Fe films deposited at 300 K (RT preparation). The hysteresis loops were recorded at 166 K. The solid and open circles denote the values obtained from curves recorded in polar and longitudinal geometry, respectively. Longitudinal curves were taken in the fcc[001] direction.

and RT preparation. No hysteresis loops could be measured below 0.9 for LT and 1.1 ML for RT films. Above these coverages the films are magnetized perpendicular to the surface and exhibit a linearly increasing saturation magnetiza-
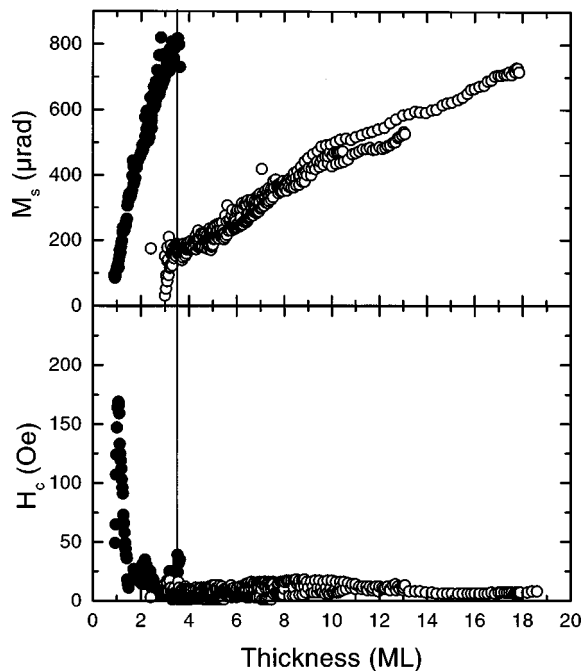

FIG. 4. Thickness dependence of the saturation magnetization M_s and of the coercive force H_c for Fe films deposited at 150 K and subsequently annealed to 300 K (LT preparation). The hysteresis loops were recorded at 166 K.
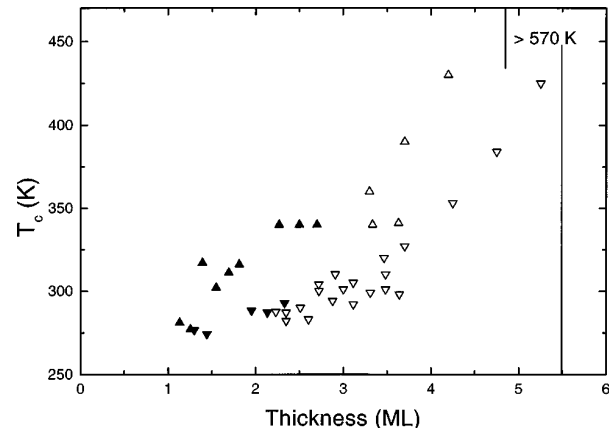

FIG. 5. Curie temperature (T_c) as a function of coverage for RT (down triangles) and LT (up triangles) preparation. The temperatures were determined from the temperature dependence of the susceptibility as described in Ref. 14. The solid and open symbols denote the values obtained from curves recorded in polar and longitudinal geometry. The perpendicular lines denote the film thickness for LT and RT films above which T_c shows a steep increase.

tion. The linear slope is typical of a homogeneously magnetized film. At a critical thickness, the magnetization switches to in plane and increases again linearly. Hence, also at these thicknesses the film is magnetized homogeneously in the film.

For an investigation of the in plane anisotropy, hysteresis curves were measured in different crystallographic directions. Below 6 ML the curves are rectangular and only a weak dependence of their shape on the in plane direction is found. Above 10 ML for RT and 5 ML for LT films, the loops get a more sigmoidal shape in fcc[001] and keep the rectangular shape in the fcc[011] direction. This development continues upon increasing coverage. Hence the easy direction above 6 ML is the fcc[011] direction. The slope and the values of the coercive force for both preparation conditions do not differ considerably from each other. The coercivity decreases from 40 Oe (1.1 ML) to 5 Oe for RT and from 170 Oe (0.9 ML) to 5 Oe for LT films.

In order to investigate the temperature dependence of the switching thickness, LT wedges were grown on the substrate and the dependence of the magnetization upon temperature was determined. The thickness, at which the hysteresis curves show a deviation from a rectangular shape and the remanence becomes smaller than the saturation magnetization, was taken as an onset for the reorientation. This investigation reveals that the switching thickness changes only in a narrow coverage regime from 3.1 ML at 300 K to 3.5 ML at 100 K. Below 3.1 ML, no longitudinal hysteresis loops were measured up to the Curie temperature. The perpendicular magnetization is stable up to the Curie temperature in this coverage regime.

The Curie temperatures for both preparation conditions are shown in Fig. 5. Below about 1 ML, no Curie temperature could be measured independent of preparation. The Curie temperature increases from 275 K at 1.2 ML to 430 K at 4.5 ML for LT and to 450 K at 5.3 ML for RT films. The values of the LT films are higher, but the difference between RT and LT films is not very pronounced. Both curves show an additional, steep increase to values above 570 K within

1 ML, whereby the onset is somewhat delayed for RT films (RT:>5.5 ML, LT:>4.5 ML).

A comparison of Figs. 3 and 4 shows that the most pronounced difference is the different stability region of the magnetic anisotropy. The perpendicular magnetization direction is observed up to 3.3 ML for LT films but only 2.3 ML for RT films. The different stability regime is also visible from the maximum value of the polar Kerr ellipticity at saturation which reaches 808 μrad for LT deposition and 520 μrad for RT preparation. This indicates that the deposition temperature affects the magnetic properties of the film. The average gradient of 240$\pm$10 μrad/ML and 223 $\pm$10 μrad/ML, respectively, for both growth conditions is fairly similiar, however.

As mentioned above, the most pronounced difference between RT and LT films is the different stability region of the perpendicular magnetization. Possibly the difference can be explained by variations in interface and surface roughness of the iron film or an interdiffusion. In order to explore if interdiffusion influences the magnetic interface anisotropies, different preparation procedures were chosen. To avoid interdiffusion at the Fe/substrate interface a homogeneous Fe film with a thickness of 2 ML was grown at 150 K. The film was annealed to 300 K for 10 min afterwards. Subsequently, a film with a wedgelike thickness distribution was deposited at 300 K. The magnetic properties of these films are shown in Fig. 6(a). Again a perpendicular magnetization at low thickness and a longitudinal one at higher coverage were found. The perpendicular magnetization reaches a maximum value of 740 μrad at 3.2 ML, the switching thickness. This behavior is comparable to that of LT films but not to RT films. The similarity implies that the interdiffusion at the Fe/substrate interface is of crucial importance. To confirm this hypothesis, a control experiment was performed where iron films were deposited and analyzed at 150 K without any annealing.

The ellipticity measured at 150 K can be compared to the values of RT and LT preparation as well as postdeposited films, because the temperature difference is only 16 K. Deposition at 150 K without subsequent annealing leads to a film whose properties closely resemble LT films [Fig. 6(b)], indicating that the surface roughness of this iron film is not crucial for the switching thickness.

Finally, we tested if the segregation of substrate atoms to the film surface could also be of importance. Therefore, 1 ML was deposited at 300 K to allow an interdiffusion at the Fe/substrate interface. Subsequently, additional Fe was grown at 150 K to avoid further diffusion. After annealing the sample to 300 K, polar and longitudinal hysteresis loops were taken at 166 K [Fig. 6(c)]. As becomes visible in Fig. 6(c), the switching thickness is comparable to films grown at 300 K but lower than the value for LT films. This similarity implies that the segregation of substrate atoms to the film surface for RT growth does not lead to a pronounced modification of the magnetic properties of the film. These experiments show that the origin of the different behavior of RT and LT films is the interdiffusion and roughness at the Fe/substrate interface rather than the roughness of the film surface and the segregation of substrate atoms to this surface. The effect of this interdiffusion of substrate and Fe atoms at
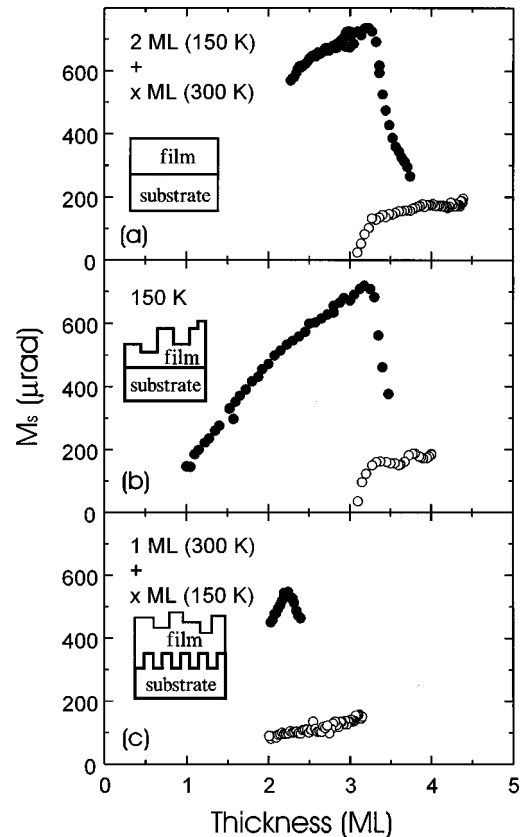

FIG. 6. M_s versus coverage for different preparation conditions: (a) after deposition of 2 ML at 150 K, subsequent annealing to 300 K and postdeposition at 300 K. Hysteresis loops were taken at 166 K. (b) after deposition at 150 K. The measurements were taken at 150 K without previous annealing. (c) after deposition of 1 ML at 300 K and growth of additional layers at 150 K followed by subsequent annealing to 300 K. Hysteresis curves were taken at 166 K. The inset describes the resulting interface and surface morphology. Solid circles denote the perpendicular magnetization, open circles denote the in-plane magnetization.

the Fe-substrate interface is a reduction of the stability regime of the perpendicular magnetization for LT films.

These results show the impact of the morphological properties on magnetic properties. In particular, roughness and diffusion at the film/substrate interface have a profound effect on these properties. However, structural changes may also influence the stability regime of the perpendicular magnetization as was shown for Fe films on Cu(100).[15,18] The existence of a perpendicular magnetic anisotropy in Fe/Cu(100) is always linked to the stabilization of the FM fcc phase, which raises the question if this phase can also be stabilized on Cu₃Au(100). Therefore we have investigated the structural properties of the films, as well.

C. Structure

The structure of the Fe films was characterized by LEED. To determine the film structure in detail, LEED I/V curves were measured and the observed LEED patterns were quantitatively analyzed. In addition, the film morphology was derived from the energy dependence of the LEED spot width.
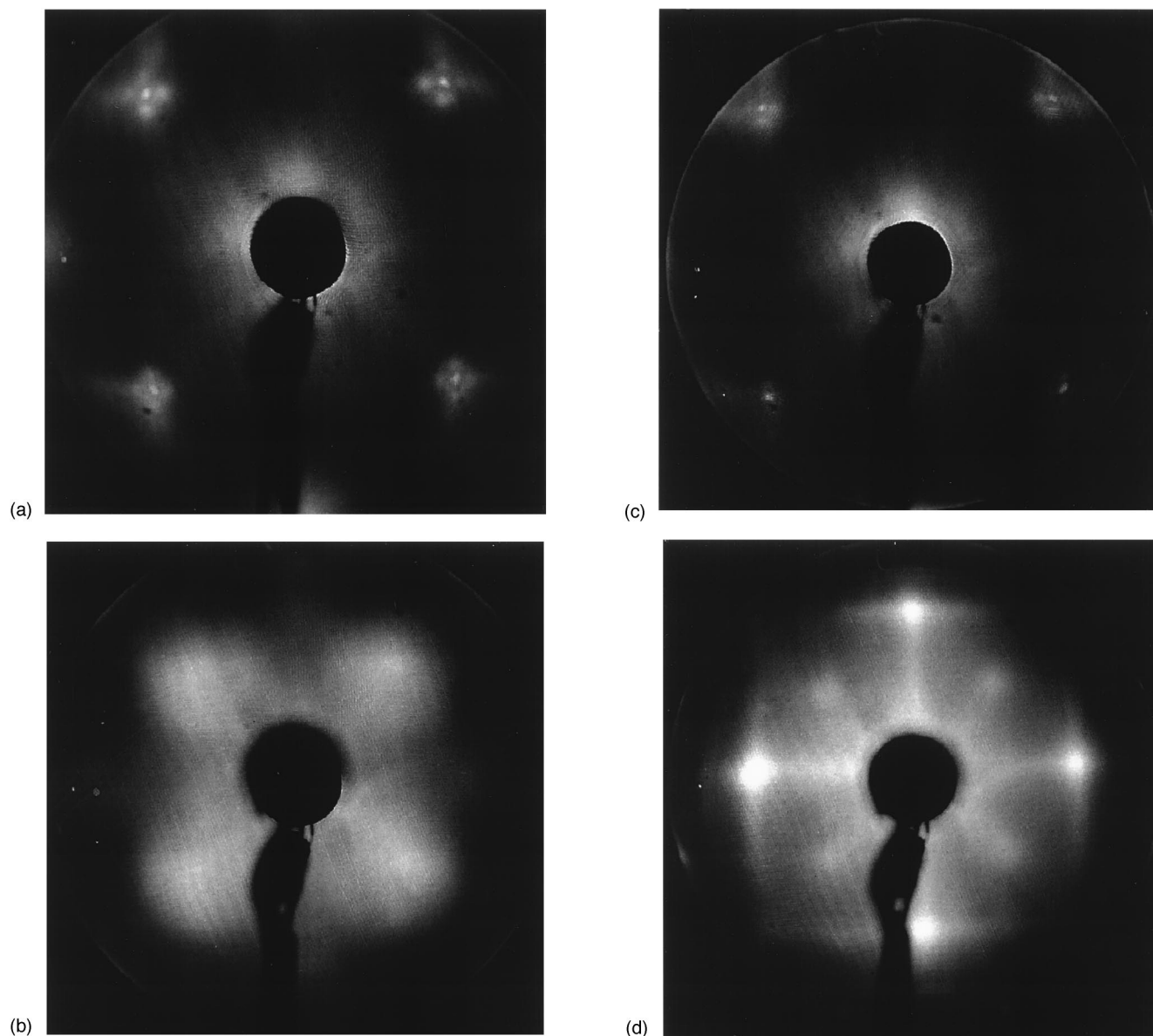
FIG. 7. LEED patterns taken at 100 K after deposition of LT films: (a) 2.2 ML ($E = 58$ eV), (b) 4.9 ML ($E = 103.5$ eV), RT films: (c) 2.7 ML ($E = 50$ eV), (d) 5.0 ML ($E = 150$ eV).

Sharp integer order spots are observed for LT films up to 3.3 ML. Above 1.2 ML, superstructure spots evolve [Fig. 7(a)]. A spot profile analysis at 1.8 ML revealed that the superstructure is either a $(n\sqrt{2} \times 1)R45$ or a $(n\sqrt{2} \times n\sqrt{2})R45$ with $n = 13$–14. Only superstructure spots around integral order beams ($k \pm 1/n, l \pm 1/n$) including $k = l = 0$ are observed. The most intense superstructure spots are always observed for the negative sign, i.e., $(k - 1/n, l - 1/n)$. Such a behavior is expected if the characteristic interatomic distance in the scattering plane is slightly larger than the nearest neighbor spacing in the $Cu_3Au(100)$ plane. Upon growing thickness, the superstructure spots converge towards the integer order spots. This can be explained by a growing superstructure unit cell. Above about 3 ML, a diffuse intensity arises around integral order spots, which becomes more intense upon growing thickness [Fig. 7(b)]. Annealing to 470 K leads to a

sharp LEED pattern and the observation of the superstructure spots up to 4.8 ML. Hence the diffuse intensity observed below 5 ML is mainly due to surface roughness. Below 5.4 ML, the LEED pattern of films deposited at 300 K exhibits also a $(n\sqrt{2} \times \sqrt{2})R45$ or a $(n\sqrt{2} \times n\sqrt{2})R45$ superstructure similar to LT films with $n = 13$–14 at 1.8 ML increasing up to 33 at 4.8 ML [Fig. 7(c)]. The superstructure spots cannot be separated from the integer order spots at about 5.5 ML. They are sharpest at low energies and become weaker at higher energy than comparable LT films. Above approximately 3 ML, additional streaks evolve running in the fcc[001] direction, which become more intense upon increasing energy and coverage [Fig. 7(d)]. Moreover, the background intensity increases at these energies. This development is observed up to 6 ML. At about 5.8 ML, the streaks in the [001] direction vanish and a very broad distributed intensity evolves around the main spots, which become more in-
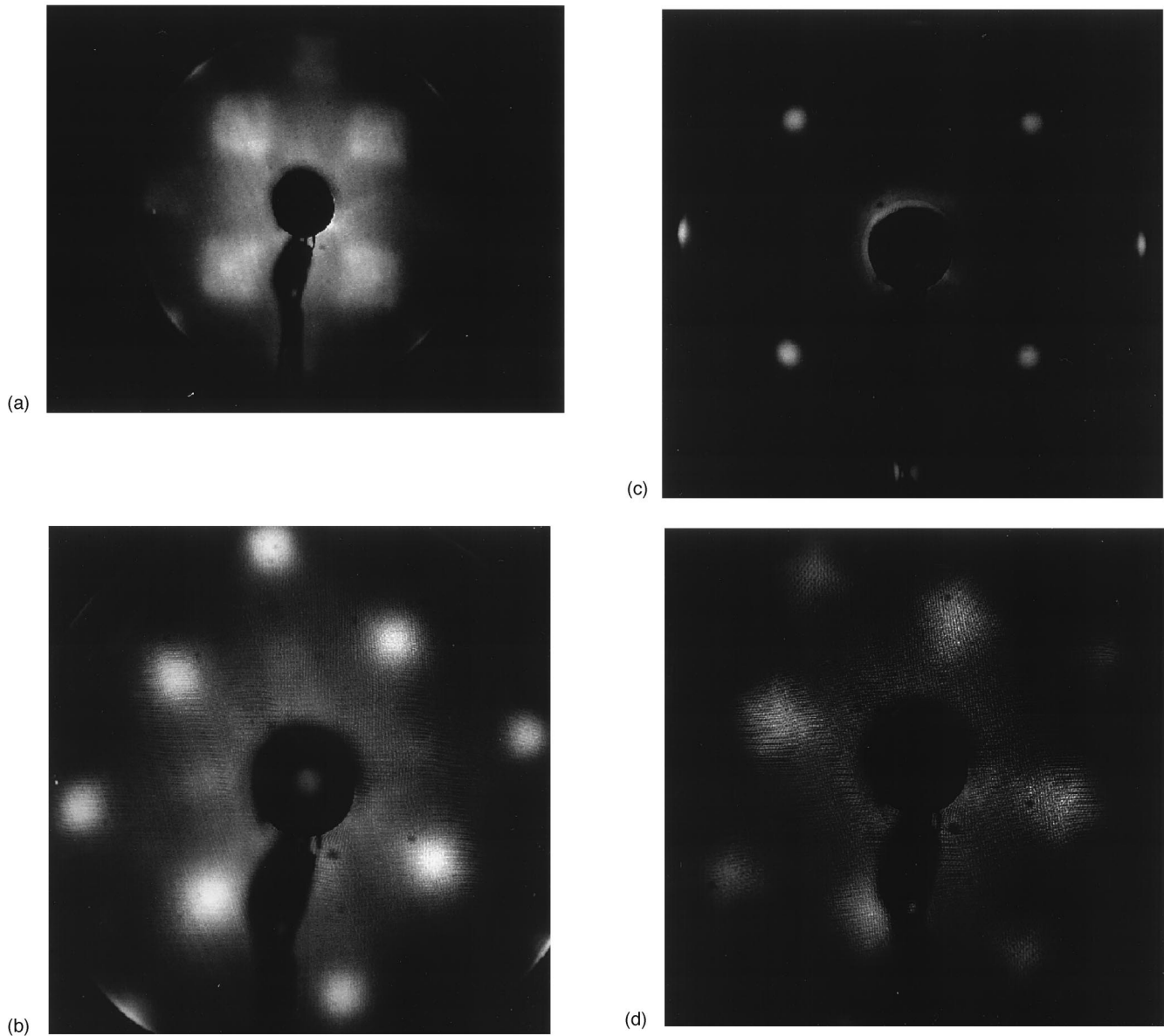
FIG. 8. LEED patterns taken at 100 K after annealing to the temperatures as denoted below of RT films: (a) 6.6 ML ($E = 93$ eV, 570 K), (b) 14 ML ($E = 94$ eV, 570 K), (c) 53 ML ($E = 57$ eV, 470 K), (d) an LT film: 8.8 ML ($E = 94.8$ eV, 570 K).

tense upon growing thickness. The intensity of integral order spots decreases and can only be observed up to 8.6 ML.

Above 9.5 ML, very broad spots remain and the LEED pattern looks similar to the pattern of LT films above 5 ML. An annealing of this phase to 570 K leads to a sharpening and the formation of a quadratic intensity distribution. In the corners of these diffuse spots an intensity enhancement is observed [Fig. 8(a)]. The centers of these spots are no longer located at the positions of the $Cu_3Au(100)$ substrate, but are located $7.6 \pm 2\%$ inwards in the fcc[011] direction in the LEED pattern. The 7.6% inward shift would correspond to a comparable expansion of the in-plane lattice constant. This leads to a next-nearest-neighbor distance of 2.87 ± 0.06 Å. The extension of these quadratic spots increases in k space with increasing energy. Therefore these LEED patterns cannot be caused by a superstructure. Only facets or mosaics can be responsible for this broadening. Spot profiles were measured to determine the angle of these facets.[19] Upon increas-

ing thickness the extension of the spots is decreasing at comparable energies, which indicates smaller angles. Finally at very large thicknesses (>30 ML), round and sharper spots are observed even after annealing the films to 470 K only [Fig. 8(c)]. No indications for faceting can be observed by LEED. Since annealing to 400 K does not improve the LEED pattern, the activation barrier for the interlayer mass transport has to be between 400 and 470 K. LT films show smaller spots already above 5 ML [Fig. 8(d)], which are comparable in quality to RT films above 10 ML after annealing. This shows that the change of the LEED pattern takes place in a smaller coverage regime than for RT-grown films.

The data presented above describe the evolution of superstructures and film morphology with growing thickness but are insufficient to determine the full structure, i.e., the precise atomic positions of the iron atoms in the film. To achieve this goal, LEED I/V curves have been recorded for several spots for a number of different thicknesses and

preparation conditions. Several of these data sets have been used as input for a full-dynamical LEED analysis. The detailed procedure and the findings of this analysis will be presented elsewhere.[20] Here we will only summarize a subset of the information obtained that is relevant to understanding the correlation between magnetic and structural properties.

The full-dynamical analysis for an annealed RT film with a coverage of 53 ML reveals an interlayer distance of 1.46 ± 0.03 Å and an in-plane lattice constant of 2.84 ± 0.05 Å. The structure of the film is unstrained bcc(100). A visual comparison with I/V curves measured for bcc Fe(001) single crystals[21,22] shows a rather good agreement as expected from the results of our full-dynamical LEED analysis. Therefore we can use the I/V curves as a fingerprint of films with a bulklike bcc(100) structure. Any structural difference in the near-surface region of films at lower thickness should result in characteristic deviations from the curves for bulklike films. Due to the high background and the diffuse spots the curves of not annealed films are of poor quality. However, the results of a quantitative analysis of a not annealed RT film at 18.7 ML yields nearly the same structural parameters as of the annealed film with a thickness of 53 ML. Hence the structure of the Fe films is already at this coverage of nearly unstrained bcc(100) Fe. The comparison with the spectra of a LT film at 6.5 ML and RT films at 8.6 and 14.4 ML reveals no significant differences between bcc(100) spectra and between each other as becomes visible in Fig. 9. Below these thicknesses, deviations from the unstrained bcc spectra are found. This can be seen in a comparison of Fig. 9(a) and 9(b). The main peaks of the I/V curves are noticeably shifted to lower energies. The shift increases upon growing energy. This can be explained by an expanded interlayer spacing in comparison to bulk bcc(100) Fe. The in-plane and the interlayer distances were determined for a 4.7 ML RT film by a quantitative LEED I/V analysis. In comparison to bulk bcc(100) Fe, the interlayer distance (1.53 ± 0.05 Å) is expanded and the in-plane distance (2.65 ± 0.06 Å) contracted. Hence the Fe grows epitaxially strained at lower coverage. These structural properties do not seem to change considerably upon decreasing coverage, because the I/V curves do not show a pronounced change down to 1.5 ML [compare Figs. 9(b) and 9(c)].

In a next step, we wanted to investigate if the preparation procedure, the segregation of Au, or a different roughness have a large impact on the film structure. For these reasons we compared LT films at 4.3 ML, RT films at 5.2 ML, and Fe films which were postdeposited by 2.7 ML at 300 K after deposition of 2 ML at 150 K [Fig. 9(b)]. The comparison of I/V curves of these films shown in Fig. 9(b) demonstrates that the structural differences are not pronounced. Therefore, different preparation procedures and the Au segregation have no profound impact on the structural properties. The I/V spectra of RT and LT films do not differ considerably upon decreasing coverage [compare Figs. 9(b) and 9(c)], which indicates a similar structure of the films for both preparation conditions at low coverage. In this thickness regime a detailed quantitative analysis of the superstructure remains as a task for future work. The superstructure spots are only visible near integral order spots including the (0,0) beam [Figs. 7(a) and 7(c)]. This restricts the number of models to a sinusoidal displacement of atoms, i.e., a corrugation of n atoms
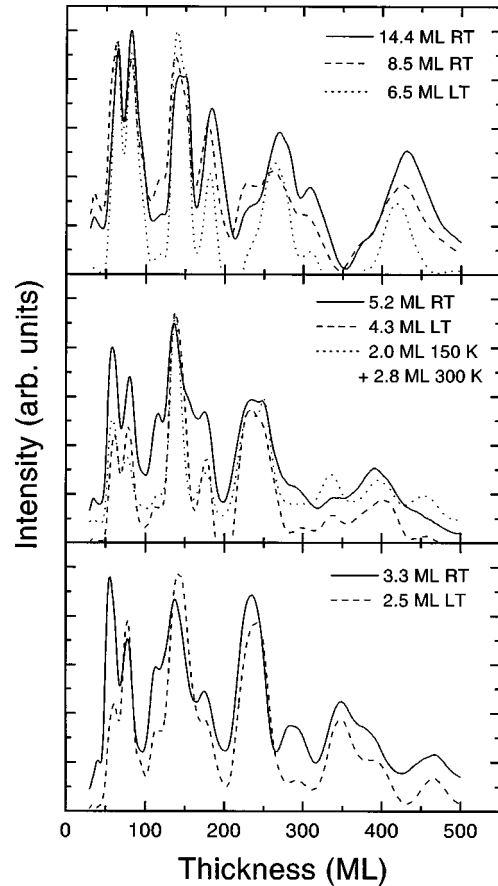

FIG. 9. Comparison between LEED I/V curves of the (0,0) spot of RT and LT films. The angle of incidence was 8° off the surface normal. (a) high coverage [RT: 14.4 ML (solid line), RT: 8.5 ML (dashed line), LT: 6.5 ML (dotted line)], (b) different preparation conditions: RT 5.2 ML (solid line), LT 4.3 ML (dashed line), postdeposited film 2 ML at 150 K + 2.8 ML at 300 K (c) low coverage: RT 3.2 ML (solid line), LT 2.5 ML (dashed line)

in the fcc[001] direction, whereby n increases from 14 at 1.8 ML to 33 for RT films at 4.8 ML. The superstructure spots do not exhibit a preferential streaking in a crystallographic orientation. Therefore we cannot distinguish if the atoms are corrugated like ''waves'' only in fcc[010] or like hillocks in both the fcc[010] and fcc[001] directions. From a kinematic simulation of the LEED pattern the corrugation amplitude can be estimated to lie between 0.2 and 0.3 Å. From these pieces of information alone it cannot be decided if only the surface atoms or the whole film is corrugated. As mentioned above, the most intense superstructure spots are observed for slightly smaller wave vectors than the substrate spots. Therefore the characteristic spacing of atoms needs to be slightly larger than 2.65 Å, the atomic spacing of the substrate layer. Hence, the corrugation may be caused by an incommensurate growth of Fe atoms, whereby n atoms occupy $n+1$ sites.

IV. DISCUSSION

A. Correlation of magnetism, structure, and morphology

For iron films grown on Cu(100) a clear correlation between magnetism, structure, and growth has been established in recent years.[3–5,23] For films grown at room temperature, a

perpendicular magnetization is observed up to approximately 10 ML. The reorientation of the magnetization at this thickness is caused by a structural transformation from an fcc-like live layer phase to bcc iron growing with the (110) orientation.[5,24] This structural transition is accompanied by a change in growth mode from layer-by-layer growth to three-dimensional growth. For deposition at low temperature, i.e., 100 to 150 K, the transition from fcc to bcc iron already takes place at around 4.5 ML and is again accompanied by a reorientation of the magnetic anisotropy.

It is tempting to try to discuss the experimental data presented here for Fe on $Cu_3Au(100)$ in a similar framework. Again, evidence is found for both a change in the magnetic and structural properties with growing film thickness. Yet, a number of findings differ considerably from the behavior observed for Fe on Cu(100). For Fe films grown on $Cu_3Au(100)$ at 300 K, a magnetic reorientation from perpendicular to in-plane is observed at 2.3 ML. For films grown at 150 K, the transition is found at 3.2 ML. This difference is caused by a different roughness of the interface as shown in Fig. 6.

Evidence for a structural change is found as well both from the analysis of the observed LEED pattern and the measurement of LEED I/V curves. These data indicate a structural change for LT films around 4.5 to 5 ML and 5.5 to 6 ML for RT films. These thicknesses are considerably larger than the critical thickness for the magnetic reorientation. Furthermore, even though the magnetic reorientation is observed at a larger thickness for LT than RT films, the structural change is observed at a lower thickness than for RT films. Confirmation for this observation comes from the measurement of T_c as a function of film thickness. Again, the steep increase of T_c with film thickness is observed with 4.8 ML for LT films earlier than for RT films (5.5 ML). This casts doubt on any attempt to relate the magnetic reorientation to a structural change, in particular a structural change from fcc to bcc iron. Yet, it is clear that the film structure at larger thickness is unstrained bcc iron. The question therefore arises what the film structure is for smaller Fe coverages between 1 and approximately 6 ML. Our LEED I/V data show signs for a structural change, but not a very pronounced one. For a structural transition from fcc to bcc iron, a considerable change in the interlayer spacing from approximately 1.75–1.9 Å for fcc iron to 1.43–1.56 Å for bcc iron is expected. This is in contrast to the results of our LEED analysis which only shows a moderate change with film thickness. Furthermore, from the LEED superstructures we conclude that the characteristic in-plane atomic spacing of the Fe atoms is 3–6 % larger than the atomic spacing in the $Cu_3Au(100)$ surface, i.e., 2.65 Å. Lin et al.[12] have recently determined an interlayer spacing of 1.9 Å for the first few iron layers from a kinematic analysis of maxima in the I/V curve of the (0,0) beam. Combining this result with a 5% expansion of the atomic spacing of the iron atoms in the plane, an atomic volume of 14.7 Å^3 is obtained. This is 20% larger than the expected atomic volume for the ferromagnetic fcc iron phase. Neglecting an expansion in the plane still produces an increase of the atomic volume by 10% compared to the ground state of ferromagnetic fcc iron. We cannot envision any mechanism which could lead to such a large

atomic volume. Hence, we have to conclude that the postulated stabilization of such an fcc iron phase is highly unplausible.

A more probable scenario is obtained if we assume the growth of a strained bcc iron modification on $Cu_3Au(100)$. For this phase an interlayer spacing of 1.65 Å is expected, in excellent agreement with the result of our LEED analysis.[20] For this phase, the misfit to $Cu_3Au(100)$ is with 7.7% quite large. Presumably, the increased atomic spacing in the iron films, which leads to the formation of superstructures, offers a mechanism to reduce the film stress. At a critical coverage, the strained bcc iron phase can no longer be stabilized and transforms to unstrained bcc iron. The transition we observe takes place at slightly different thickness depending upon growth temperature and is observed at a smaller thickness for LT films. Such an observation is plausible as well. The mixing at the interface for RT films should lead to a gradient in composition which could reduce the overall stress and increase the critical thickness for dislocation formation. The observed structural change is therefore mainly controlled by the elastic properties of the film, the misfit to the substrate, and the interface properties. The magnetic reorientation is unrelated to the structural change. The reorientation thickness is caused by a competition of crystal and shape anisotropy. The interface anisotropy can be modified considerably by an intermixing at the interface which explains the dependence of the magnetic reorientation upon growth temperature.

B. Comparison with previous studies

The longitudinal magnetization at film thicknesses above 3 to 5 ML has already been observed by a number of authors.[10–12,25,26] Keune et al.[25] and Macedo et al.[26] investigated the magnetic properties of Fe films grown on $Cu_3Au(100)$ at 473 and 309 K by Mössbauer spectroscopy. At 5 ML the magnetization direction is orientated in the film plane. A remanent, in-plane magnetization was found at room temperature by Rochow et al.[10] only above 3.6 ML from spin-resolved electron energy-loss experiments. The magnetic reorientation from perpendicular to in plane was observed by Baudelet et al.[11] A recent paper by Lin et al.[12] attributes this to a structural change from fcc to bcc iron. A similar structural change has already been postulated by Rochow et al.[10] Both findings were derived from a kinematic analysis of the LEED I/V maxima of the (0,0) beam. We believe that for the iron films on $Cu_3Au(100)$ only a full-dynamical analysis of an extended data set with several beams can lead to reliable data. We have performed such an analysis and find evidence for a strained bcc modification below approximately 4–5 ML. Above this thickness a structural change to unstrained bcc iron is observed. A structural change in this transition regime has also been observed in the STM studies of Lin et al.[12] Again, the observed change in film morphology, in particular, in step height as a function of film thickness has been attributed to a transition from fcc to bcc iron. We believe that this change in step height can also be explained by a transition from strained to unstrained bcc iron in the entire film, which should change the step height between strained und unstrained areas by approximately 0.4 Å. This is in agreement with the observations of Lin et al.

Hence, the phase transition from strained to unstrained bcc iron appears to be consistent with the experimental data presented so far.

V. SUMMARY

A correlation between the magnetic, structural, and morphological properties of ultrathin Fe films on $Cu_3Au(100)$ was established for LT and RT preparation. Below 5 ML for LT and 5.5 ML for RT films the Fe grows epitaxially strained with a tetragonally distorted bcc(100) modification. The films exhibit a buckling with an amplitude of about 0.2 Å in the fcc[001] direction, which seems to be caused by an incommensurate growth. The periodicity of the buckling increases upon growing thickness.

The magnetization is oriented perpendicular to the film plane above 1 ML. RT films switch to in-plane at 2.3 ML, LT films at 3.3 ML. The perpendicular magnetization is stable up to the Curie temperature and can be detected for LT films up to 3.1 ML at 300 K. The different switching thicknesses are a result of an interdiffusion of Fe and substrate atoms at the Fe-substrate interface, i.e., an occupation of Fe atoms at subsurface sites. This decreases the interfacial anisotropy. Predominantly Au atoms segregate on top of the film surface during deposition at 300 K and are partly incorporated in the film upon growing coverage. Above 4.8 ML for LT and 5.5 ML for RT films the film relaxes to unstrained bcc(100) Fe. The transition regime for RT films lies between 5.5 and 10 ML and is larger than for LT films. This transition also changes the magneto-optic properties of the Fe film. Yet, the structural transition is unrelated to the magnetic reorientation observed at smaller thickness.

[1] U. Gradmann, in *Magnetism In Ultrathin Transition Metal Films*, edited by K. H. J. Buschow (Elsevier Science, Amsterdam, 1993), Vol. 7, Chap. 1, pp. 74–96.

[2] E. F. Wassermann, *IFF-Ferienschule, Magnetismus von Festkörpern und Grenzflächen* (Forschungszentrum Jülich GmbH, Jülich, 1993), Vol. 24.

[3] S. Müller, P. Bayer, C. Reischl, K. Heinz, B. Feldmann, H. Zillgen, and M. Wuttig, Phys. Rev. Lett. **74**, 765 (1995).

[4] R. D. Ellerbrock, A. Fuest, A. Schatz, W. Keune, and R. A. Brand, Phys. Rev. Lett. **74**, 3053 (1995).

[5] J. Thomassen, F. May, B. Feldmann, M. Wuttig, and H. Ibach, Phys. Rev. Lett. **69**, 3831 (1992).

[6] D. Li, M. Freitag, J. Pearson, Z. Q. Qiu, and S. D. Bader, J. Appl. Phys. **76**, 6425 (1994).

[7] G. L. Krasko and G. B. Olson, Phys. Rev. B **40**, 11 536 (1989).

[8] S. D. Bader and E. R. Moog, J. Appl. Phys. **61**, 3729 (1987).

[9] M. Stampanoni, A. Vaterlaus, M. Aeschlimann, and F. Meier, Phys. Rev. Lett. **59**, 2483 (1987).

[10] R. Rochow, C. Carbone, T. Dodt, F. P. Johnen, and E. Kisker, Phys. Rev. B **41**, 3426 (1990).

[11] F. Baudelet, M.-T. Lin, W. Kuch, K. Meinel, B. Choi, C. M. Schneider, and J. Kirschner, Phys. Rev. B **51**, 12 563 (1995).

[12] M.-T. Lin, J. Shen, W. Kuch, H. Jenniches, M. Klaua, C. M. Schneider, and J. Kirschner, Phys. Rev. B **55**, 5886 (1997).

[13] J. Thomassen, B. Feldmann, and M. Wuttig, Surf. Sci. **264**, 406 (1992).

[14] A. Berger, S. Knappmann, and H. P. Oepen, J. Appl. Phys. **75**, 5598 (1994).

[15] M. Wuttig, H. Zillgen, and B. Feldmann, Surf. Sci. **321**, 32 (1994).

[16] G. Tréglia and B. Legrand, Phys. Rev. B **35**, 4338 (1987).

[17] H. Okamato, T. B. Massalski, L. J. Swartzendruber, and P. A. Beck, Bull. Alloy Phase Diagrams **5**, 592 (1984).

[18] M. Wuttig, B. Feldmann, and T. Flores, Surf. Sci. **331–333**, 659 (1995).

[19] B. Feldmann, Ph.D. thesis, Forschungszentrum Jülich, 1996.

[20] B. Schirmer, B. Feldmann, and M. Wuttig (unpublished).

[21] K. O. Legg, F. Jona, D. W. Jepsen, and P. M. Marcus, J. Phys. C **10**, 937 (1977).

[22] Z. Q. Wang, Y. S. Li, and F. Jona, Solid State Commun. **61**, 623 (1987).

[23] D. Li, M. Freitag, J. Pearson, Z. Q. Qiu, and S. D. Bader, Phys. Rev. Lett. **72**, 3112 (1994).

[24] K. Kalki, D. D. Chambliss, K. E. Johnson, R. J. Wilson, and S. Chiang, Phys. Rev. B **48**, 18 344 (1993).

[25] W. Keune, T. Ezawa, W. A. A. Macedo, U. Glos, and U. Kirschbaum, Physica B **161**, 269 (1989).

[26] W. A. A. Macedo, W. Keune, and E. D. Ellerbrock, J. Magn. Magn. Mater. **93**, 552 (1991).